Forest Chemicals Review
www.forestchemicalsreview.com
ISSN: 1520-0191
May-June 2022 Page No. 794-805
Article History: Received: 24 February 2022, Revised: 05 April 2022, Accepted: 08 May 2022, Publication: 30 June 2022

# System Identification of Air Cushion Vehicle Motion Model Based on EKF

**Jianbo Xiao[1], Xuming Liu[2], Yucheng Ma[1,3]**
[1]College of Naval Architecture & Ocean Engineering, Naval University of Engineering, Wuhan, 430033, China
[2]Unit 91202 of PLA, Huludao, 125004, China
[3]Unit 91999 of PLA, Qingdao, 266400, China

***Abstract:***

The motion model of air cushion vehicle is the foundation for analyzing its maneuvering characteristics and design training simulation system. The motion model can be affected by the mutual coupling of multiple factors, is difficult to established. In this paper, the method of estimating the parameters of the nonlinear system by the extend Kalman filter (EKF) is introduced. According to separate modeling method, combined with aerodynamics and hydrodynamics, the model of form-drag (moment), Aerodynamic force (moment), hydrodynamic force (moment), propeller propulsion force (moment), rudder force (moment), and force (moment) generated by side wind gates are generated. The known parameters of LCAC are substituted into the MMG model for Z-shaped simulation test to estimate the feasibility of EKF in identifying the parameters of air cushion vehicle motion model. And the results show that the method can be practical to use in system identification of air cushion vehicle motion model.

***Keywords****: Extended Kalman filter, MMG modeling, Motion mode, System identification, Simulation, Air cushion vehicle.*

As a kind of advanced technology and highly versatile water carrier platform, air cushion vehicle is widely used in modern sea battlefield and has bright prospects for development. However, it has characters such as many operating equipments, complex control system and fast speed, makes it difficult to operate. The regular sea training has many disadvantages such as high costs, long training cycle, low efficiency and high risk. In order to save equipment maintenance support and training funds, shorten the training cycle of the crew member, extend the service life of equipment, make up for the shortage of practical training, ensure training safety and broaden the training content, it is urgent to develop a supporting simulation training system. Based on the expansion of Kalman filter, the manipulation motion model parameter identification is carried out, the three degrees of freedom movement model of ACV is established, the simulation results of three degrees of freedom model for direct flight and swing test show that the model can be very good in simulation the direct flight movement and the swing movement below the moderate rudder.

The ACV movement model is the key to the ACV's operation simulation training system, and the inaccuracy of the model will cause the trainee to form the wrong operating habits in the course of training, which will lead to negative training effects. How to obtain accurate model parameters and establish a

*Forest Chemicals Review*
*www.forestchemicalsreview.com*
*ISSN: 1520-0191*
*May-June 2022 Page No. 794-805*
*Article History: Received: 24 February 2022, Revised: 05 April 2022, Accepted: 08 May 2022, Publication: 30 June 2022*

model in line with the real law of motion has become an urgent problem to break through. Identification modeling is a modeling method of estimating the mathematical model of the process by taking the input and output data of the subject process being studied and processing and calculating it as necessary[1,2]. Based on the ACV manipulation motion separation model, this paper uses the extended Kalman filter (EKF) to identify some unknown fluid dynamic parameters in the separation model, and the parameter identification and system identification are equivalent. Due to the lack of real boat manipulation test data, this paper uses the U.S. LCAC boat parameters[3] to carry out Z-shaped manipulation simulation test on the ACV, and takes the simulation test results as the sample data of identification modeling, so as to verify the feasibility of EKF in identifying the parameters of the ACV manipulation model.

## I. SYSTEM IDENTIFICATION MODELING

System identification modeling refers to obtaining the inherent parameters of a system based on a recognition algorithm when the input (e.g. rudder excitation) and output (e.g. transposing response) are known**Error! Reference source not found.**. Zadeh defines system identification as follows: based on input and output data, a model equivalent to the system under test is determined from a given set of model classes[0]. By this definition, identification can be summed up in three elements: data, models, and guidelines. Taking the model of air cushion boat manipulation as an example, the principle of identification is Fig 1. Data is the physical basis for identification, and under the experimental conditions of the design, measuring the input and output sequences [u(k), y(k), k=1, 2, ..., N] of the specified system is the required data. Experimental conditions should ensure that the input signal can fully excite all the mods of the process, so as to identify the higher precision model parameters. The selection of model M depends on the a priori knowledge of the researchers, which can be a separate model or a whole model, and a separate model is selected in this paper. Guideline C, also known as loss function, is a function about the output error ε(k), the system identification is actually through the identification algorithm L to optimize the loss function, so that it tends to minimize, the resulting parameter estimation $\hat{\theta}$ will make M and the motion process P (i.e. the actual law) fit best.

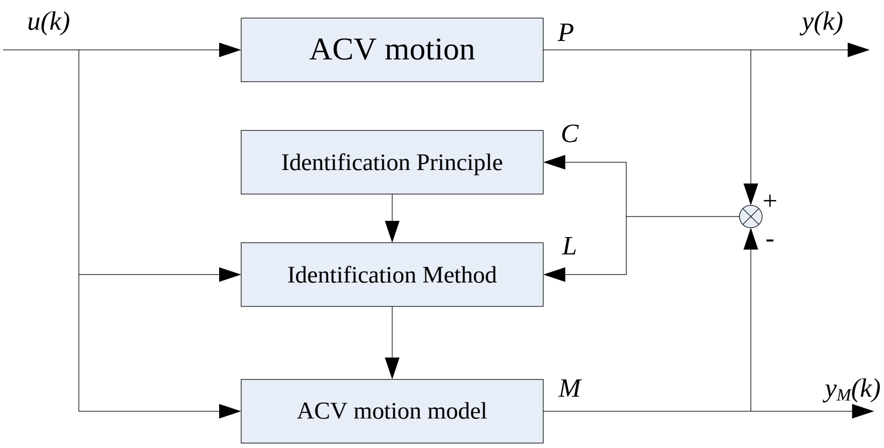


Fig 1: Schematic diagram of system identification for ACV motion

Forest Chemicals Review
www.forestchemicalsreview.com
ISSN: 1520-0191
May-June 2022 Page No. 794-805
Article History: Received: 24 February 2022, Revised: 05 April 2022, Accepted: 08 May 2022, Publication: 30 June 2022

## II. EXTENDED KALMAN FILTER

Common identification algorithms include the smallest diplication, (extended) Kalman filtering, and artificial neural network algorithms. The least squared method is the most basic and widely used method, but the method cannot be applied directly to the parameter estimation of the state spatial form model**Error! Reference source not found.**. Kalman filtering is suitable for linear models, and for nonlinear models, extended Kalman filtering is required to identify**Error! Reference source not found.**. Artificial neural networks can theoretically approximate any nonlinear function[0], be suitable for black box modeling**Error! Reference source not found.**, or estimate parameters by calculating weights, which is similar to the minimum diplication. This section focuses on the extended Kalman filter and its application in the identification of parameters of the ACV motion model.

### 2.1 Kalman Filter

The dynamic nature of physical processes can be described in a state space method. For a deterministic linear non-time-change system

$$\begin{aligned}\dot{X}(t) &= AX(t) + BU(t) \\ Y(t) &= CX(t)\end{aligned} \tag{1}$$

Among them, *A* is the system matrix, *B* is the input matrix, *C* is the output matrix, all three are time-independent constants, *X(t)* is the state vector, *U(t)* is the input (control) vector, and *Y (t)* is the output (measurement) vector. Discrete treatment of formula (1), can get the follows:

$$\begin{aligned}X(k+1) &= \Phi X(k) + GU(k) \\ Y(k) &= CX(k)\end{aligned} \tag{2}$$

There into

$$\begin{aligned}\Phi &= e^{Ah} \\ G &= \left(\int_0^h e^{At} dt\right) B\end{aligned} \tag{3}$$

*h* is the sampling period.

In the actual system, there are often various kinds of interference, then the actual system equation is as the follow:

Forest Chemicals Review
www.forestchemicalsreview.com
ISSN: 1520-0191
May-June 2022 Page No. 794-805
Article History: Received: 24 February 2022, Revised: 05 April 2022, Accepted: 08 May 2022, Publication: 30 June 2022

$$\begin{aligned} \dot{X}(t) &= AX(t) + BU(t) + w(t) \\ Y(t) &= CX(t) + v(t) \end{aligned} \tag{4}$$

Wherein, *w(t)* is system noise and *v(t)* is measured noise, both of which conform to Gaussian distribution. After the same discrete processing, we can get the follows:

$$\begin{aligned} X(k+1) &= \Phi X(k) + GU(k) + w(k) \\ Y(k) &= CX(k) + v(k) \end{aligned} \tag{5}$$

The system noise sequence {*w(k)*} is caused by interference from the external environment (e.g. wind and waves in ship motion), while the measured noise sequence {*v(k)*} is caused by thermal noise inside the measuring instrument (sensor). Both are random, so the system is random at this time. Kalman filters perform best in this regard in order to estimate state vector *X(k)* as accurately as possible. Set up a series of measurement data $Y(1),Y(2),\cdots,Y(j),k\geq j$,use the vector $Y_j$ to indicate, that is

$$Y_j = \left[ Y(1) \;\; Y(2) \;\; \cdots \;\; Y(j) \right]^T \tag{6}$$

The resulting state vector estimate is recorded as $\hat{X}(k|j)$, and the corresponding estimation error is $\tilde{X}(k|j) = X(k) - \hat{X}(k|j)$, because $\tilde{X}(k|j)$ is also random, the state estimation criterion needs to be defined from a statistical point of view, and then the optimal state estimate $\hat{X}(k|j)$ is obtained by minimizing the criterion. Using the mean square $\tilde{X}(k|j)$ as the criterion example, the error mean square and the extreme value method are treated minimally.

$$J = E\left[ \tilde{X}^T(k|j)\tilde{X}(k|j) \right]_{Y_j} \tag{7}$$

$$\min J \rightarrow dJ / d\hat{X}(k|j) = 0 \tag{8}$$

After Calculation:

$$\hat{X}(k|j) = \int_{-\infty}^{+\infty} X(k) f_{X|Y_j}\left[ X(k)|Y_j \right] dX(k) = E\left[ X(k)|Y_j \right] \tag{9}$$

2.2 Extended Kalman Filter

If the fluid dynamic parameters to be identified are added to the state vector of the system, the formula (5) becomes

Forest Chemicals Review
www.forestchemicalsreview.com
ISSN: 1520-0191
May-June 2022 Page No. 794-805
Article History: Received: 24 February 2022, Revised: 05 April 2022, Accepted: 08 May 2022, Publication: 30 June 2022

$$X'(k+1)=\begin{bmatrix} X(k+1) \\ \Theta \end{bmatrix}=\varphi\left[X'(k),U(k)\right]+w(k) \\ Y(k)=h\left[X'(k)\right]+v(k) \tag{10}$$

Among them, $X'(k+1)$ is the augmented state vector, $\Theta$ is all the parameters to be identified, this is the EKF model. To estimate the state and parameters of a nonlinear system, it needs to be linearized. Linearizes $\varphi\left[X'(k),U(k)\right]$ in the neighborhood of $\tilde{X}'(k)$

$$\varphi[X'(k),U(k)]=\varphi\left[\hat{X}'(k),U(k)\ \right]+\frac{\partial\varphi}{\partial X'}\bigg|_{X'=X'(k)}\cdot\left(X'(k)-\hat{X}'(k)\right) \tag{11}$$

Linearizes $h\left[X'(k)\right]$ in the neighborhood of $\hat{X}'(k|k-1)$

$$h[X'(k)]=h\left[\hat{X}'(k|k-1)\right]+\frac{\partial h}{\partial X'}\bigg|_{X'=\hat{X}'(k|k-1)}\cdot\left(X'(k)-\hat{X}'(k|k-1)\right) \tag{12}$$

If we make the following equals:

$$\begin{gathered}\frac{\partial\varphi}{\partial X}=\Phi(k) \\ \varphi[X'(k),U(k)]-\frac{\partial\varphi}{\partial X'}\bigg|_{X'=X'(k)}\cdot X'(k)=M(k) \\ \frac{\partial h}{\partial X'}\bigg|_{X'=\hat{X}'(k|k-1)}=C(k) \\ h\left[\hat{X}'(k|k-1)\right]+\frac{\partial h}{\partial X'}\bigg|_{X'=\hat{X}'(k|k-1)}\cdot\hat{X}'(k|k-1)=N(k)\end{gathered} \tag{13}$$

We can get the linearized system equation as follow:

$$X'(k+1)=\Phi(k)X'(k)+M(k)+w(k) \\ y(k)=C(k)X(k)+N(k)+v(k) \tag{14}$$

At this point, KF's filtering formula can be referenced, and the series formulas of the EKF can be sorted out

$$\hat{X}'(k+1|k)=\varphi[\hat{X}'(k),U(k)\ ] \\ \hat{X}'(k+1)=\hat{X}'(k+1|k)+K(k+1)\{y(k+1)-h[\hat{X}'(k+1|k)]\} \\ K(k+1)=P(k+1|k)C^T(k+1)\cdot[C(k+1)P(k+1|k)C^T(k+1)+R(k+1)]^{-1} \tag{15}$$

Forest Chemicals Review
www.forestchemicalsreview.com
ISSN: 1520-0191
May-June 2022 Page No. 794-805
Article History: Received: 24 February 2022, Revised: 05 April 2022, Accepted: 08 May 2022, Publication: 30 June 2022

$$P(k+1|k) = \Phi(k)P(k)\Phi^{\mathrm{T}}(k) + Q(k)$$
$$P(k+1) = [I - K(k+1)C(k+1)P(k+1|k)]$$

There into

$$\Phi(k) = \frac{\partial \varphi}{\partial X'}\bigg|_{X'=\hat{X}'(k)} = \begin{pmatrix} \hat{\Theta} & \hat{X}'(k) \\ 0 & 1 \end{pmatrix} \tag{16}$$

*K* is the filter gain, *P* is the prediction mean square error, *R* and *Q* are the ANOVA matrix of measured noise and system noise, *I* is the unit matrix, by the use of formula (15), $\Theta$ can be estimated.

## III. BASED ON EKF'S ACV MODEL PARAMETER IDENTIFICATION

It is very complicated to apply EKF to identify the parameters of the six-degree-of-freedom motion model of ACV. Because there are too many parameters and there is a great possibility of elimination effect between the parameters, it is not realistic to identify all the parameters accurately. Therefore, in this paper, three degrees of freedom motion model is used. There is only one variable, the rudder angle, as the input of the system.

### 3.1 Three Degrees of Freedom Separation Model of ACV

In order to facilitate calculation, the motion model of ACV is reduced to three degrees of freedom model

$$\begin{aligned} m(\dot{u} - vr) &= X_A + X_H + X_P + X_R \\ m(\dot{v} + ur) &= Y_A + Y_H + Y_R \\ I_z \dot{r} &= N_A + N_H + N_R \end{aligned} \tag{17}$$

Among them, the subscript *A* is for aerodynamic, *H* is for hydrodynamic, *P* is for propeller force, *R* is for rudder force, and $I_z$ if for the inertia of the ACV to the Z axis of the motion coordinate system. With the parameters $\Theta$ to be identified, the model equation of EKF can be obtained:

$$\begin{aligned} \dot{u} &= f_1(u, v, r, \delta, \Theta)/m + vr \\ \dot{v} &= f_2(u, v, r, \delta, \Theta)/m - ur \\ \dot{r} &= f_3(u, v, r, \delta, \Theta)/I_z \\ \dot{\psi} &= r \\ \dot{\Theta} &= 0 \end{aligned} \tag{18}$$

Forest Chemicals Review
www.forestchemicalsreview.com
ISSN: 1520-0191
May-June 2022 Page No. 794-805
Article History: Received: 24 February 2022, Revised: 05 April 2022, Accepted: 08 May 2022, Publication: 30 June 2022

As can be seen from formula (18), the parameters identified in this paper are constant. Therefore, the force and torque in the right side of the formula (17) equation need to be processed. Using the representation method in the reference [11], wherein aerodynamics can be expressed as follows:

$$\begin{aligned} X_A &= X_{Au}u + X_{Auu}u^2 + X_{Avv}v^2 + X_{Auv}uv \\ Y_A &= Y_{Av}v + Y_{Avv}v^2 + Y_{Auv}uv \\ N_A &= N_{Av}v + N_{Ar}r + N_{Avvv}v^3 + N_{Arrr}r^3 + N_{Avvr}v^2 r + N_{Avrr}vr^2 \end{aligned} \tag{19}$$

Hydrodynamics can be expressed as:

$$\begin{aligned} X_H &= X_{H\dot{u}}\dot{u} + X_{Hu}u + X_{Huu}u^2 + X_{Hvv}v^2 + X_{Huv}uv \\ Y_H &= Y_{H\dot{v}}\dot{v} + Y_{Hv}v + Y_{Hvv}v^2 + Y_{Huv}uv \\ N_H &= N_{H\dot{v}}\dot{v} + N_{Hv}v + N_{Hr}r + N_{H\beta}\beta + N_{Hvvv}v^3 + N_{Hrrr}r^3 + N_{Hvvr}v^2 r + N_{Hvrr}vr^2 \end{aligned} \tag{20}$$

According to the theory of parameter identification**Error! Reference source not found.**, wherein, $X_{H\dot{u}}$, $Y_{H\dot{v}}$, $N_{H\dot{v}}$ and other inertial force derivatives do not participate in identification, can be calculated by slender body theory. Portrait and lateral forces can be expressed as:

$$\begin{aligned} X_R &= -3(C_{R1} + C_{R2}|\delta| + C_{R3}\delta^2)S_r p_{ri} \\ Y_R &= -3C_{R4}\delta S_r p_{ri} \end{aligned} \tag{21}$$

The parameter estimates can then be made by replacing the formula (19), the formula (20) and the formula (21) with the formula (17).

### 3.2 Parameter Identification Results and Analysis

In this paper, the batch parameter identification is used, first of all, the simulation model is used to carry out the mild test, that is, 5°/5° Z-shaped test, identify the linear item parameters, with the moderate test and the severe test that is 15°/15° and 25°/25° Z-shaped test to identify the nonlinear item parameters. According to the data of 3 kinds of experimental simulation results, the parameter identification results are shown in Table 1. The overall identification results are consistent with the parameters of the simulation model, in which the linear item parameters are more accurate and the nonlinear parameters are less accurate. This is because the mild test can make the ACV basically in the linear range of motion, and although the moderate test and the heavy test can make the ACV carry out nonlinear movement, but the different nonlinear parameters of the nonlinear parameters of the nonlinear movement of the contribution is different, the greater the contribution, the higher the recognition accuracy. To improve the accuracy of nonlinear parameter recognition, the sensitivity of nonlinear parameters needs to be analyzed in more depth.

Forest Chemicals Review
www.forestchemicalsreview.com
ISSN: 1520-0191
May-June 2022 Page No. 794-805
Article History: Received: 24 February 2022, Revised: 05 April 2022, Accepted: 08 May 2022, Publication: 30 June 2022

**TABLE I. Hydrodynamic coefficient**

| Hydrodynamic coefficient | relative error | absolute error | Hydrodynamic coefficient | relative error | absolute error |
|---|---|---|---|---|---|
| $X_{Au}$ | 5.60250 | -1.094% | $N_{Avvv}$ | 4.26350 | -20.000% |
| $X_{Auu}$ | 4.37870 | -18.408% | $N_{Arrr}$ | -70.70850 | 20.000% |
| $X_{Avv}$ | -0.99780 | -10.000% | $N_{Avvr}$ | 11.28450 | -20.000% |
| $X_{Auv}$ | -0.89950 | 10.000% | $N_{Avrr}$ | 28.41690 | -19.320% |
| $X_{Hu}$ | 9.28630 | -1.912% | $N_{Hv}$ | 12.68730 | -2.000% |
| $X_{Huu}$ | 1.46550 | -10.001% | $N_{Hr}$ | 4.24660 | -2.000% |
| $X_{Hvv}$ | -0.57990 | -14.994% | $N_{H\beta}$ | 7.31280 | -2.000% |
| $X_{Huv}$ | 1.12040 | -20.000% | $N_{Hvvv}$ | 3.37230 | -20.000% |
| $Y_{Av}$ | -14.65480 | 2.587% | $N_{Hrrr}$ | 52.44740 | -19.626% |
| $Y_{Avv}$ | 15.01490 | -18.745% | $N_{Hvvr}$ | 8.21830 | -20.000% |
| $Y_{Auv}$ | -84.40640 | 20.000% | $N_{Hvrr}$ | 18.25520 | -20.000% |
| $Y_{Hv}$ | -3.13940 | 0.619% | $C_{R1}$ | -0.00020 | -2.083% |
| $Y_{Hvv}$ | 10.08140 | -20.000% | $C_{R2}$ | -0.00006 | -5.172% |
| $Y_{Huv}$ | 59.68650 | -19.043% | $C_{R3}$ | -0.00013 | -39.940% |
| $N_{Av}$ | 0.04560 | -2.004% | $C_{R4}$ | -0.00037 | -2.331% |
| $N_{Ar}$ | 5.74240 | -2.000% | | | |

## IV. MECHANISM MODELING SIMULATION

Based on the three degrees of freedom motion model described above, this section simulates the linear motion and swing motion.

In the actual ACV full cushion lift navigation state, the wind will have the greatest impact, the simulation test selected wind as an environmental variable. Using pulsation winds with wind direction and wind speed changing over time, the direction of wind direction changes within ±5 degrees, and wind speed changes within ±1m/s. The amount of variation is generated using Gaussian white noise, plus the set wind direction and wind speed to get the wind model.

(1) ACV swing movement without wind conditions

To carry out the swing test below the moderate rudder angle, the rudder angle is: 5 degrees, 8 degrees, 10 degrees, 13 degrees and 15 degrees a total of 5 different rudder angles, the initial position of the ACV in

Forest Chemicals Review
www.forestchemicalsreview.com
ISSN: 1520-0191
May-June 2022 Page No. 794-805
Article History: Received: 24 February 2022, Revised: 05 April 2022, Accepted: 08 May 2022, Publication: 30 June 2022

the simulation is the origin, the initial speed is 30 knots, the initial direction is positive northward, in the steering process to maintain the speed of the air propeller unchanged, the external environment conditions are windless.

Fig 2 is the swing motion simulation trajectory of the ACV at different rudder angles, the diamond point in the figure is the starting point of the ACV's swing motion, and it can be seen from the figure that the steering angle changes from small to large, and the swing radius of the ACV is gradually reduced, in line with the general law of the ACV's swing motion.

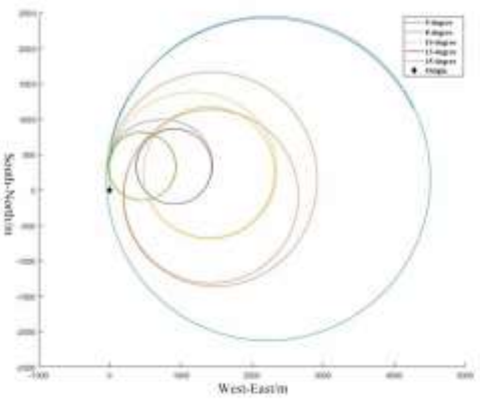


Fig 2: The ACV swings the motion simulation track

Fig 3 is the speed of ACV in different rudder angle swing simulation, from the figure can be seen, with the increase of rudder angle, the speed of the speed decreased in turn, in line with the ACV in the swing process of the change of the law of speed.

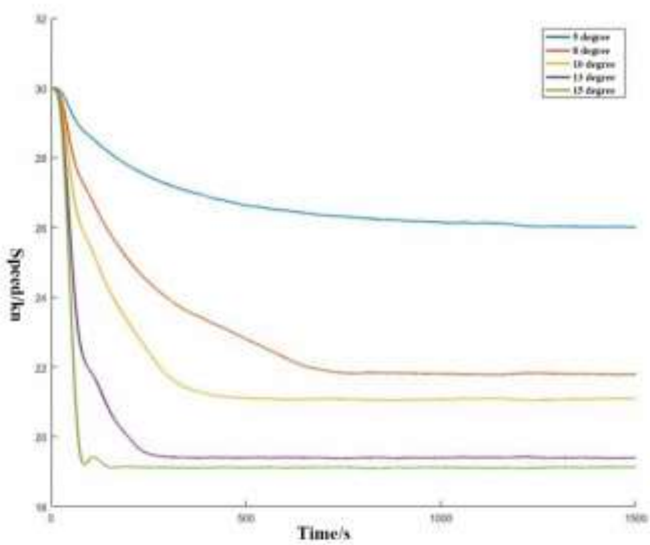


Fig 3: The speed of ACV swing motion

*Forest Chemicals Review*
*www.forestchemicalsreview.com*
*ISSN: 1520-0191*
*May-June 2022 Page No. 794-805*
*Article History: Received: 24 February 2022, Revised: 05 April 2022, Accepted: 08 May 2022, Publication: 30 June 2022*

Fig 4 is the speed of the swing angle of the motion simulation of the ACV, and it can be seen from the figure that the larger the swing rudder angle, the greater the speed of the ACV's swing angle, which is consistent with the change of the ACV's general swing angle speed.

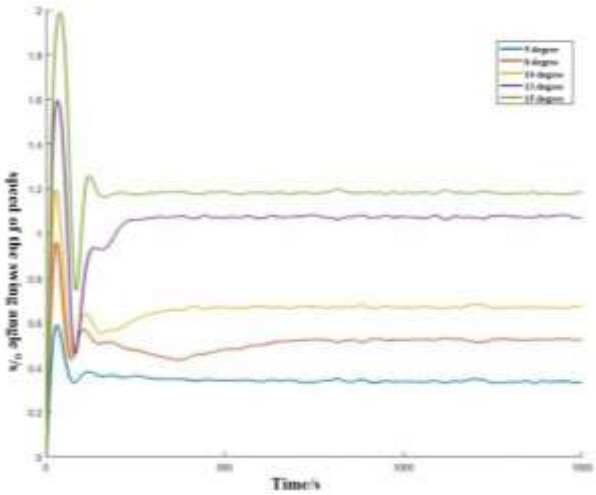

Fig 4: The speed of the swing angle of the ACV in swing motion

From the swing test below the moderate rudder of the ACV, it can be seen that under the condition of no wind, the change law of the swing motion trajectory, speed, angular velocity and other parameters with the swing rudder angle is in line with the law of the ACV movement, and it can be proved that the model established can theoretically reflect the swing test of the ACV below the moderate rudder angle without wind conditions.

(2) ACV swing movement with wind conditions

Considering that the steering angle of this model is not easy to be too large, the corresponding setting of wind speed is not easy to be too large, wind conditions of the swing simulation test conditions are divided into two: First, 15 degrees rudder angle, wind speed of 2m/s, wind angle is 0 degrees, 45 The wind speed is 2m/s, the wind angle is 0 degrees unchanged, and the rudder angle is 5, 8, 10, 13 and 15 degrees respectively.

Under the first cond e same
during the voyage, chai ulation
track Fig 5 shows. It ca ed will
reduce the swing radius change
the direction of the AC on is in
line with the objective l

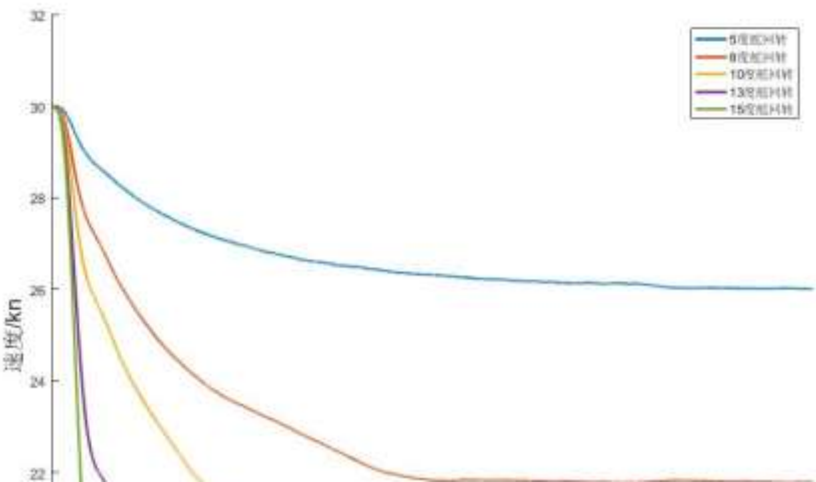

*Forest Chemicals Review*
*www.forestchemicalsreview.com*
*ISSN: 1520-0191*
*May-June 2022 Page No. 794-805*
*Article History: Received: 24 February 2022, Revised: 05 April 2022, Accepted: 08 May 2022, Publication: 30 June 2022*

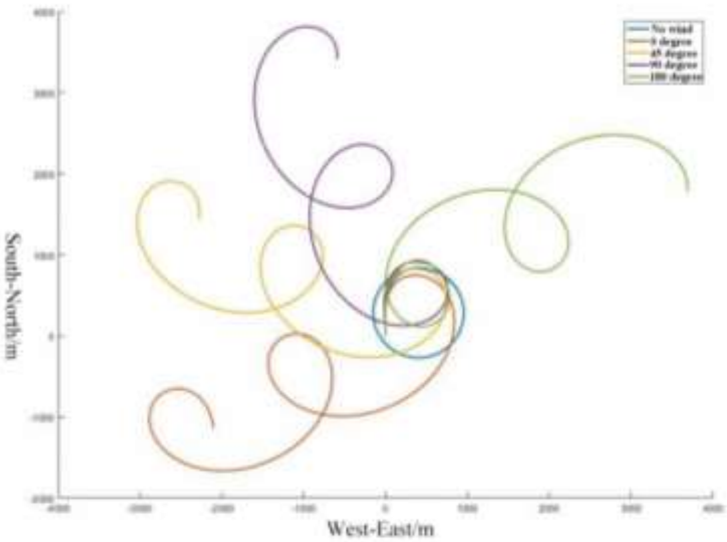


Fig 5: The simulation trajectory of the ACV swing

Under the second condition, the initial speed of the ACV is 30 knots, the propeller speed remains the same during the voyage, changing the rudder angle, and the swing simulation trajectory is shown in Fig 6.

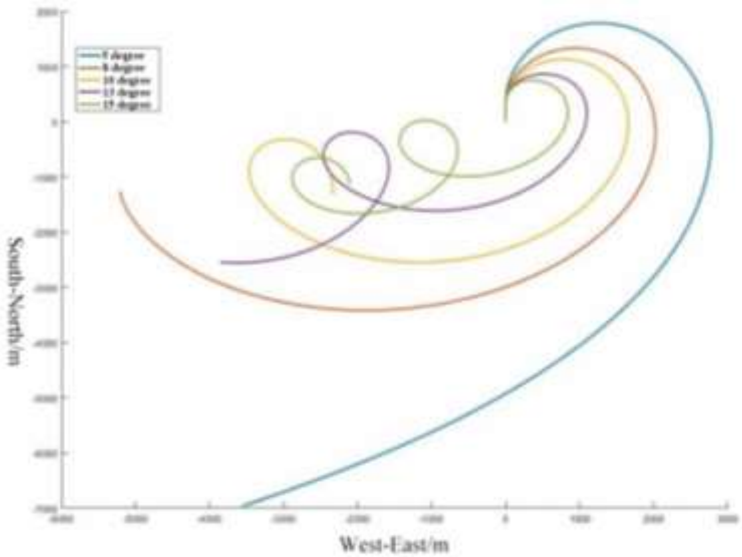


Fig 6: The simulation trajectory of the ACV swing in different rudder angle

As can be seen from Figure 6, under the same wind speed and wind direction, with the increase of rudder angle, the radius of the ACV's rotation will decrease, the easier the swing, when the wind speed is relative to the ACV's speed is too large, the final track of the ACV will tend to be straight line; In the case of the same wind speed, wind direction and rudder angle, when the ACV is turned from the sailing state of the headwind to the wind, the radius of the swing will be smaller, the radius of the swing will be smaller when the wind direction is turned into the headwind state, and even when the wind speed is too large

*Forest Chemicals Review*
*www.forestchemicalsreview.com*
*ISSN: 1520-0191*
*May-June 2022 Page No. 794-805*
*Article History: Received: 24 February 2022, Revised: 05 April 2022, Accepted: 08 May 2022, Publication: 30 June 2022*

relative to the rudder angle, The ACV cannot be turned from a downwind state to a headwind. From a qualitative point of view, the model can be built to simulate the ACV in wind conditions below the moderate rudder angle of the swing test.

## V. CONCLUSION

In view of the characteristics of high training cost, long cycle, low efficiency and high loss of air cushion vehicle training, it is urgent to develop a matching training simulation system. In order to solve the problem of motion model accuracy in training simulation system, three degree of freedom separation model of ACV is established according to MMG separation modeling thought. The principle of system identification is analyzed, and the formula of EKF identifying nonlinear model parameters is derived. Comparing the identified parameters with the parameters of the simulation model, the EKF's identification ACV motion model is finally verified.

## REFERENCES

[1] Zhang XG. Identification modeling based on analysis of ship maneuvering tests. Shanghai: Shanghai Jiao Tong University, 2012.
[2] Wang XG. On the modeling of ship maneuvering motion in 4 degrees of freedom based on support vector machines. Shanghai: Shanghai Jiao Tong University, 2014.
[3] Damon C, et al. Mathematical Model of an Air Cushion Vehicle. AD-A015 699, Cambridge: Charles Stark Draper Lab, 1975.
[4] Tian YF, Huang LW, Xiong Y, et al. Parameter identification of ship motion model by using novel bat algorithm. Science Technology and Engineering, 2018, 18(8):136-143.
[5] Zadeh LA. From circuit theory to system theory. Proceedings of the Institute of Radio Engineers, 1962, 50(5):856-865.
[6] Bai WW, Ren JS, Li TS, et al. Locally optimal-based LWL identification modeling for ship maneuvering motion. Journal of Harbin Engineering University, 2017, 38(5):676-683.
[7] Huo C, Dong WC. Identification of ship roll parameters form free-roll decay based on extended Kalman filtering. Journal of Wuhan University of Technology (Transportation Science & Engineering), 2016, 40(2):214-226.
[8] Sandberg IW. Structure theorems for nonlinear systems. Multidimensional Systems and Signal Processing, 1991, 2(3):267-286.
[9] Xiao JB, Hu DB, Liu XM. Research on hovercraft manipulation motion model parameter identification based on extend Kalman filter. Modern Electronics Technique, 2020, 43(2):110-114.
[10] Xu F, Zou ZJ, Xu XK, et al. Black-box modeling of ship maneuvering motion based onsupport vector machines. Journal of Beijing University of Aeronautics and Astronautics, 2013, 39(11):1553-1557.
[11] Li WJ. Study on the instructional system of air cushion vehicle simulator. Harbin: Harbin Engineering University, 2010.
[12] Luo WL, Li TS, Zou ZJ. Parametric identifiability in modeling of ship maneuveringmotion. Journal of Dalian Maritime University, 2009, 35(4): 1-3.